Journal of Molecular Structure 1173 (2018) 697–706

Contents lists available at ScienceDirect

Journal of Molecular Structure

journal homepage: http://www.elsevier.com/locate/molstruc

The first Fe(II) complex bearing end-to-end dicyanamide as a double bridging ligand: Crystallography study and Hirshfeld surface analysis; completed with a CSD survey

Zouaoui Setifi [a, b], David Geiger [c], Christian Jelsch [d], Thierry Maris [e], Christopher Glidewell [f], Masoud Mirzaei [g, *], Mina Arefian [g], Fatima Setifi [a]

[a] Laboratoire de Chimie, Ingénierie Moléculaire et Nanostructures (LCIMN), Université Ferhat Abbas Sétif 1, Sétif 19000, Algeria
[b] Département de Technologie, Faculté de Technologie, Université 20 Août, 1955–Skikda, Skikda 21000, Algeria
[c] Department of Chemistry, SUNY-College at Geneseo, Geneseo, NY 14454, USA
[d] CRM², CNRS, Institut Jean Barriol, Université de Lorraine, Vandoeuvre les Nancy, France
[e] Département de Chimie, Université de Montréal, 2900 Boulevard Edouard-Montpetit, Montréal, Québec H3C 3J7, Canada
[f] School of Chemistry, University of St Andrews, Fife KY16 9ST, United Kingdom
[g] Department of Chemistry, Faculty of Science, Ferdowsi University of Mashhad, Mashhad, Iran

ARTICLE INFO

Article history:
Received 9 May 2018
Received in revised form
28 June 2018
Accepted 13 July 2018
Available online 17 July 2018

Keywords:
Crystal engineering
Iron
Dicyanamide
Double bridge
Hirshfeld surface analysis

ABSTRACT

Two new polymeric, one and two-dimensional compounds [Fe(dmbpy) ($\mu_{1,5}$-dca)$_2$] (**1**) and [Fe(4,4′-bpy) ($\mu_{1,5}$-dca)$_2$].0.24(4,4′-bpy).0.5(EtOH) (**2**), in which dmbpy = 5,5′-dimethyl-bipyridine, dca = dicyanamide and 4,4′-bpy = 4,4′-bipyridine, has been synthesized under solvothermal conditions and fully characterized by elemental analysis, FT-IR spectroscopy and X-ray single crystal diffraction. Compound **1**, with a rare coordination environment, is the only well-known example in which end-to-end double bridged dca ligands and a bidentate bulky aromatic ligand (dmbpy) are coordinated simultaneously to the iron center. Structural analysis of compound **2** showed it is a novel two-dimensional coordination polymer, constructed from repetition of 4,4′-bpy and dca as a bidentate bridging ligand. Changing the co-ligand to 4,4′-bpy, lead to completely different structure geometry and network, which confirms the substantial effect of co-ligand. Furthermore, Hirshfeld surfaces analyses have been performed to help understand the packing.

1. Introduction

The field of crystal engineering of metal–organic structures is of particular modern researches, in order to obtainvarious compounds with multidimensional networks [1–4]. Among different trends of complexes of transition metals, compounds with N-donor bridging ligands are of special importance due to their ability to form infinite polymeric frameworks [3]. These compounds display rich structural and topological features and exhibit physical properties ranging from conductivity to magnetism [4].

Recently, polynitrile and pseudohalide ligands, have proven to be very versatile and diverse in different areas such as coordination chemistry and molecular materials chemistry [5–16]. In particular, the pseudohalide ligand dicyanamide, hereafter dca, with the formula of $[N(CN)_2]^-$ received considerable attention because of its various modes of coordination character and bridging ability [17,18]. It is a well-known building block to form 1D and 2D frameworks due to its flexible nature and various modes of coordination. Moreover, since the dca ligand is an anionic ligand, no other anions are required in the structure to balance the charge [19].

Different coordination and bridging modes of dca as a ligand are illustrated by its four distinct structures in Scheme 1. Part (I) exhibits monodentate coordination mode through a nitrile nitrogen atom, (II) bidentate (μ_2) is related to end-to-end bridging mode through the two nitrile nitrogen atoms, (III) tris-monodentate (μ_3) bridging of three metal atom and (IV) which is very similar to that of (II), except that a pair of dca ligands makes a double bridge between two metal centers. The third coordination mode, μ_3, observed in several neutral 3D compounds with the general formula of $[M^{II}(dca)_2]$ in which M(II) is Fe, Mn, Co, Ni or Cu, which exhibit a rutile-like structure [3,20–22].

* Corresponding author.
E-mail addresses: mirzaeesh@um.ac.ir (M. Mirzaei), fat_setifi@yahoo.fr (F. Setifi).

https://doi.org/10.1016/j.molstruc.2018.07.049
0022-2860/

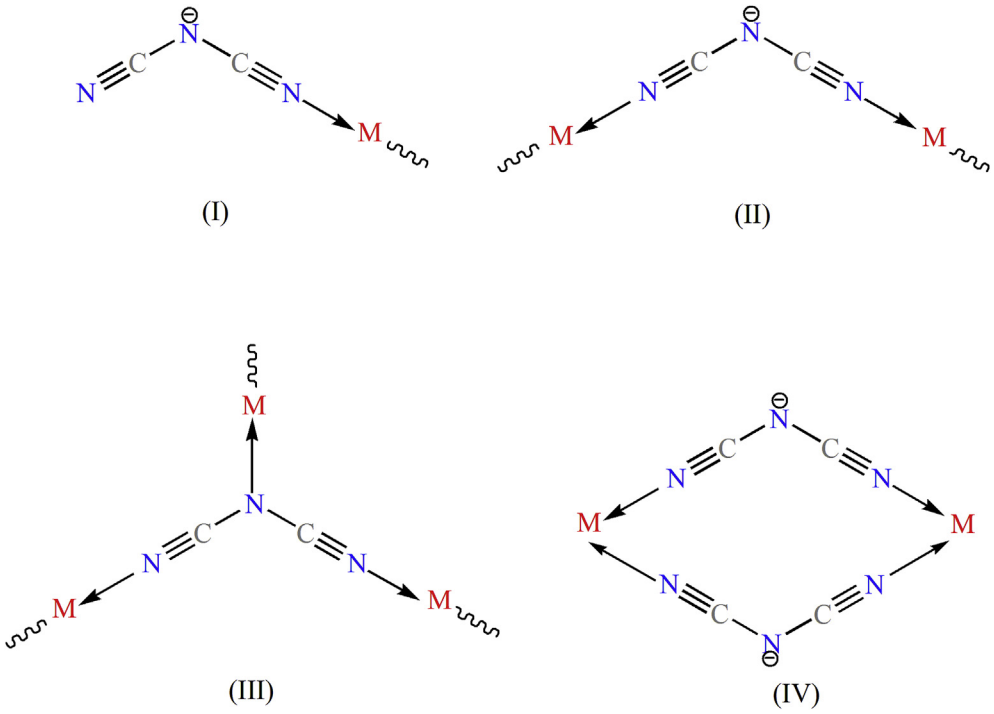

Scheme 1. Different coordination modes of dca as single bridging ligand in: (I) mondentate, (II) bidentate, (III) tridentate and as double bridging mode in (IV).

Lower dimensional systems with general formula $[M(L)_2(dca)_4]$, where L is monodentate ligand, have also been reported by coordination of two blocking L ligands. In this case the four remaining coordination sites are occupied by the nitrogen atoms of the dca ligands, leading to square two-dimensional systems with each metal center bridged by means of four single end-to-end dca to four neighboring ones [23–25], or one-dimensional systems with double end-to-end dca bridges along the chains [26,27].

A Cambridge Structural Database (CSD) search on various types of coordination modes of dca ligand with iron metal center in Scheme 2 indicates the rarely occurring double bridge mode, in which each pair of dca ligand bridges two iron atoms (Scheme 1; Part IV).

The structures and networks of the coordination polymers of dca can be strongly modified by the introduction of co-ligands [28]. In this research we focused on the bipyridine family of N-donor ligand (4,4′-bpy and dmbpy), as co-ligand. Two different novel polymeric network structures based on iron complexes of dca and dmbpy were synthesized successfully. Using dca along with 4,4′-bpy ligand leads to polymeric planes in compound **2**, while exploiting another member of bipyridine ligands, dmbpy, resulted in an absolutely different network. The CSD survey revealed that compound **1** has a rare coordination environment. This compound and the manganese complex (*cis*-[Mn(bpy) $(N(CN)_2)_2]_n$) [29] are the only examples in which end-to-end double bridged dca ligands and a bidentate bulky aromatic ligand such as 4,4′-bpy are coordinated simultaneously to the metal center, while in other similar structures, the coordination of a bidendate aromatic ligand prevents the formation of the double bridged dca ligands and only one pair of dca ligands act as a mono-bridge between the metal centers [4,30,31].

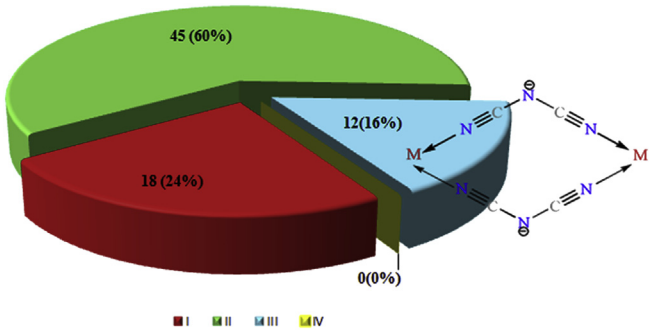

Scheme 2. Distribution of different coordination modes of dca with iron metal center based on CSD investigation. (Blue part emphasizes the lower number of illustrated double bridge end-to-end mode, on histogram).

2. Experimental

2.1. Materials and physical measurements

All the reagents and solvents employed were commercially available and used as received without further purification. Elemental analyses (C, H and N) were performed using a Perkin-Elmer 2400 series II CHN analyser. Infrared spectra were recorded in the range of 4000–500 cm^{-1} on a FT-IR Bruker ATR Vertex 70 Spectrometer.

2.2. Synthesis and crystal growth

2.2.1. Synthesis of [Fe(dmbpy) ($\mu_{1,5}$-dca)$_2$] (1)

A mixture of $FeSO_4 \cdot 7H_2O$ (0.2 mmol, 56 mg), dmbpy (0.2 mmol, 37 mg) and Nadca (0.4 mmol, 36 mg) in H_2O/EtOH (1:1 *v/v*, 10 mL) was heated at 453 K for 2 days in a sealed Teflon-lined stainless-steel vessel under autogenous pressure and then gradually cooled to room temperature at a rate of 10 K h^{-1}. After the reaction vessel was cooled to ambient temperature, orange crystals of **1** were obtained with a yield of 25%. Anal. Calcd. for **1**: C, 51.63; H, 3.25; N, 30.11. Found: C, 51.92; H, 3.19; N, 30.43%. Selected IR bands (ν/cm^{-1}): ν_s(C≡N) 2180(vs); ν_{as}(C≡N) 2239(m); ν_{as}(C≡N) + ν_s(C≡N) 2304 (m).

Table 1
Crystal data and structure refinement parameters of complexes **1** and **2**.

	Complex 1	Complex 2
Crystal data		
Chemical formula	$C_{16}H_{12}FeN_8$	$2(C_{14}H_8FeN_8).0.4815(C_{10}H_8N_2)\cdot C_2H_6O$
M_r	372.19	809.54
Crystal system, space group	Monoclinic, *C*2/*c*	Monoclinic, *C*2/*m*
Temperature (K)	293	200
a, *b*, *c* (Å)	7.427 (5), 16.682 (5), 13.601 (5)	19.908 (9), 14.944 (8), 12.194 (6)
α, β, γ (°)	90, 96.413 (5), 90	90, 91.379 (18), 90
V (Å^3)	1674.6 (14)	3627 (3)
Z	4	4
Radiation type	Mo Kα	Mo Kα
μ (mm^{-1})	0.917	0.856
Crystal size (mm)	0.35 × 0.20 × 0.11	0.50 × 0.50 × 0.30
Data collection		
Diffractometer	Bruker APEXII CCD	Bruker SMART X2S
Absorption correction	Multi-scan (*SADABS*; Bruker, 2013)	Multi-scan (*SADABS*; Bruker, 2013)
T_{min}, T_{max}	0.832, 0.902	0.815, 0.843
No. of measured, independent and observed [$I > 2\sigma(I)$] reflections	9653, 2452, 1928	15510, 3794, 2246
R_{int}	0.027	0.047
$(\sin\theta/\lambda)_{max}$ (Å^{-1})	0.706	0.625
Refinement		
$R[F^2 > 2\sigma(F^2)]$, $wR(F^2)$, S	0.033, 0.094, 1.05	0.043, 0.125, 1.04
No. of reflections	2452	3794
No. of parameters	115	280
No. of restraints	0	65
H-atom treatment	H-atom parameters constrained	H-atom parameters constrained
$\Delta\rho_{max}$, $\Delta\rho_{min}$ (e Å^{-3})	0.36, −0.21	0.66, −0.41

2.2.2. Synthesis of [Fe(4,4′-bpy)($\mu_{1,5}$-dca)$_2$].0.24(4,4′-bpy).0.5(EtOH) (2)

Prepared under similar conditions to that of complex **1**, except that 4,4′-bpy (0.2 mmol, 31 mg) was used instead of dmbpy. Orange crystals of **2** were obtained with a yield of 20%. Anal. Calcd. for **2**: C, 51.66; H, 3.22; N, 29.34. Found: C, 51.92; H, 3.19; N, 30.43%. Selected IR bands (ν/cm^{-1}): ν_s(C≡N) 2187(vs); ν_{as}(C≡N) 2244(m); ν_{as}(C≡N) + ν_s(C≡N) 2307 (m).

2.3. X-ray crystallography

Details of crystal data, data-collection and refinement parameters are given in Table 1: standard software packages were used throughout [32–34], and full details of the refinement procedures, including the handling of the disorder in **2**, are provided in the Supporting Information. The refined occupancy of the uncoordinated 4,4′-bipy unit in **2** is 0.963(6) and the occupancies of the two ethanol components are 0.694(9) and 0.306(9).

3. Results and discussion

3.1. Crystal structure description

3.1.1. [Fe(dmbpy) ($\mu_{1,5}$-dca)$_2$]$_n$ (1)

A perspective view of a section of complex **1** together with the atom numbering scheme is presented in Fig. 1, and selected bond parameters are summarized in Table S1 (Supplementary section).

This compound is best described as a one-dimensional chain coordination polymer. In the structure of **1**, the [(dmbpy)Fe] units lie across two-fold rotation axes in space group *C*2/*c*, with the reference unit selected as that lying across the axis along (½, y, ¼). Monomeric units of this type are linked by pairs of inversion-related dicyanamide ligands, forming chains of spiro-fused 12-membered rings along the [001] direction (Fig. 2).

The geometry around the iron(II) ion is distorted octahedral with the *xy* plane formed by the two nitrogen atoms of the bidentate dmbpy ligand (Fe1–N11 = 2.2122(14) Å) and two nitrogen atoms of symmetry-related bridging dicyanamide anions (Fe–N21 = 2.1308(17) Å). Although similar structure observed previously with Mn as metal center [29], but this is the first structure, in which end-to-end double bridged dca ligands and a dmbpy ligand are coordinated simultaneously to Fe center. The angular restriction imposed by the dmbpy ligand (N11–Fe1–N11^i = 74.16°, see Table S1 for symmetry descriptors) results in a widened angle between the *trans* dca ligands (N21–Fe1–N21^i = 101.51°). The axial positions are occupied by nitrogen atoms of the other bridging dca anions with Fe1–N25^{ii} = 2.1666(18) Å and decidedly nonlinear N25^{iv}-Fe1-N25^{ii} = 171.55(8)°. The Fe1···Fe1 distance within the chain is 7.481(2) Å and the shortest Fe1···Fe1 distance between chains is 9.130(3) Å.

The Fe–N distances in **1** indicate that the Fe(II) adopts a HS (high spin) configuration. Thus the unique Fe–N(dmbpy) distance 2.2122(14) Å is close to Fe–N(pyridyl) distances in other HS complexes [35,36], and the two Fe–N(dca) distances are of similar magnitude to the Fe–N(dmbpy) distance. By contrast, in LS (low spin) Fe(II) complexes of 2,2′-bipyridine and 1,10-phenanthroline,

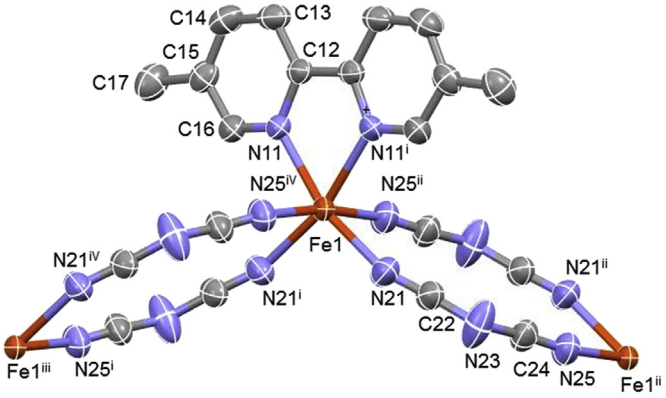

Fig. 1. Perspective view of a section of 1 together with partial atom numbering Symmetry codes: (i) −x + 1, y, -z + ½; (ii) -x + 1, -y + 1, -z + 1; (iii) −x + 1, -y + 1, -z; (iv) x, -y + 1, z − ½.

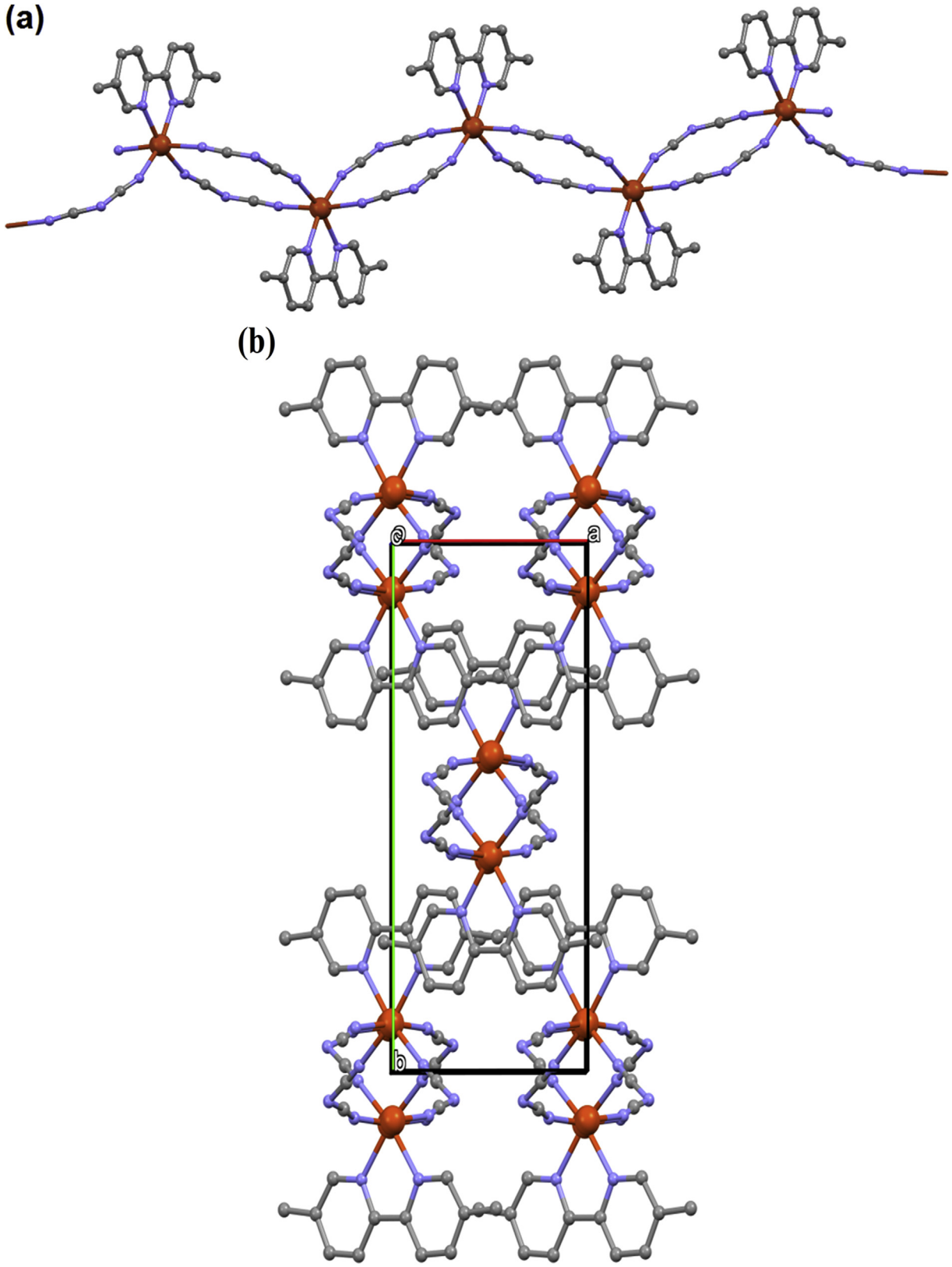

Fig. 2. The crystal structure of compound 1, showing (a) the formation of a coordination polymer chain along [001] and (b) the arrangement of the chains on a centred rectangular grid. The H atoms have all been omitted for clarity.

the Fe–N distances are all close to 1.97 Å [37–39]. For comparison, an analysis of interatomic distances in simple salts indicated a difference of ca. 0.16 Å in effective radius between HS octahedral Fe(II) and the corresponding LS counterpart [40].

3.1.2. *[Fe(4,4′-bpy) ($\mu_{1,5}$-dca)$_2$]$_n$ 0.0.24(4,4′-bpy).0.5(EtOH) (2)*

Complex **2** (perspective view is shown in Fig. 3 and selected bond lengths and bond angles are summarized in Table S2, which are in good agreement with similar coordination compounds containing dca and dmbpy ligands [41]) crystallizes as a two-dimensional coordination polymer in space group *C*2/*m*. One pair of *trans* coordination sites at the octahedral Fe center is occupied by two independent 4,4′-bipy ligands. One of these lies across the two-fold rotation axis along (1/2, *y*, 0) and so bridges the two Fe centers at (*x*, *y*, *z*) and (1 - *x*, *y*, 2 - *z*), while the other lies across the two-fold rotation axis along (0, *y*, ½), so linking the Fe centers at (*x*, *y*, *z*) and (-*x*, *y*, 1 - *z*). In this way a chain of composition [Fe(4,4′-bipy)]$_n$ is formed, running parallel to the [101] direction. The other four coordination sites are occupied by the terminal N atoms of four independent dca ligands, all of which lie across mirror planes. One pair of dca units, occupying mutually *cis* sites lie across the mirror plane at $y = 0$, so linking the Fe centers at (*x*, *y*, *z*) and (*x*, -*y*, *z*), while the second pair lie across the mirror plane at $y = 0.5$, linking the Fe centers at (*x*, *y*, *z*) and (*x*, 1- *y*, *z*). These interactions form a chain of spiro-fused 12-membered rings of composition [Fe(dca)$_2$]$_n$ running parallel to the [010] direction.

The combination of the [010] and [101] chains generates an almost planar sheet, in the form of a (4,4) net lying parallel to (10–1) and having composition [Fe(4,4′-bipy) (dca)$_2$]$_n$ (Fig. 4).

Two sheets of this type, related to one another by the C-centring operation, pass through each unit cell, but these sheets occupy only ca. 75% of the available volume of the unit-cell. The sheets enclose two pairs of voids, one pair centred at (0, 0, ½) and (½, ½, ½) each having a volume of ca. 250 Å^3, and a second pair centred at (½, 0, ½) and (0, ½, ½) with a volume of ca. 215 Å^3. Each of the larger voids is occupied by an uncoordinated 4,4′-bipy unit, lying on a site of 2/m (C_{2h}) symmetry and having occupancy 0.963(6). Each of the smaller voids is occupied by an inversion-related pair of ethanol molecules, each disordered over two sets of atomic sites having occupancies 0.694(9) and 0.306(9). Hence the overall composition of this material is 4[Fe(4,4′-bipy) (dca)$_2$].0.963(4,4′-bipy).2(EtOH).

The composition of the coordination polymer sheets indicates that iron is present as Fe(II), and the Fe–N distances indicate that the Fe(II) adopts a HS configuration. Thus, the Fe–N(4,4′-bipy) distances 2.209(2) Å and 2.227(2) Å are close to Fe–N(pyridyl) distances in other HS complexes [35,36], and the Fe–N(dca) distances, which are closely clustered around 2.15 Å are of similar magnitude to the Fe–N(4,4′-bipy) distances here. By contrast, in low-spin Fe(II) complexes of 2,2′-bipy and 1,10-phen, the Fe–N distances are all close to 1.97 Å [37–39]. For comparison, an analysis of interatomic distances in simple salts indicated a difference of ca. 0.16 Å in effective radius between HS octahedral Fe(II) and the corresponding LS counterpart [40].

Within the sheets, the two independent Fe···Fe distances bridged by the dca ligands are 7.447(3) Å and 7.497(3) Å, while those across the 4,4′-bipy bridges are 11.533(4) Å and 11.583(4) Å (Fig. 5).

3.2. Infrared spectroscopy

The IR spectra of the dicyanamido compounds are quite similar and exhibit strong to medium absorptions in the 2320-2110 cm^{-1} region corresponding to the ν(C≡N) stretching frequencies of the dca ligand. In both complexes, the frequencies are shifted to higher values compared to the free dca. These results are in agreement with the literature for coordinated dca ligand [42].

3.3. Hirshfeld surface and enrichment ratio

Compound 1. The Hirshfeld surface analysis was undertaken to further characterize the intermolecular contacts. The

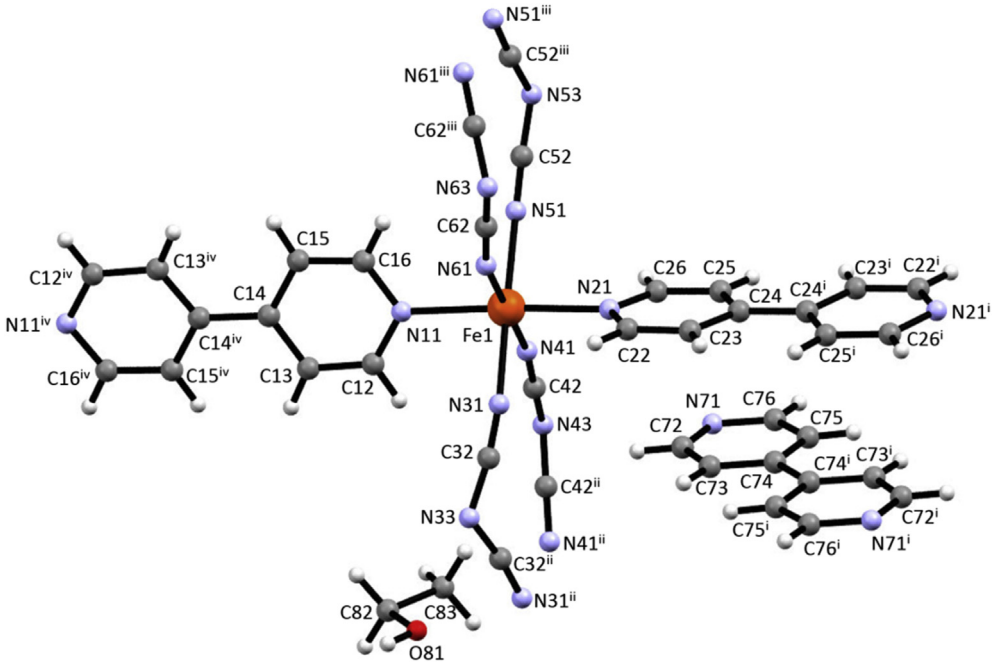

Fig. 3. Perspective view of a section of 2 together with partial atom numbering. Symmetry codes: (i) -x, y, -z + 1; (ii) x, -y, z; (iii) x, -y + 1, z; (iv) −x +1, y, -z + 2.

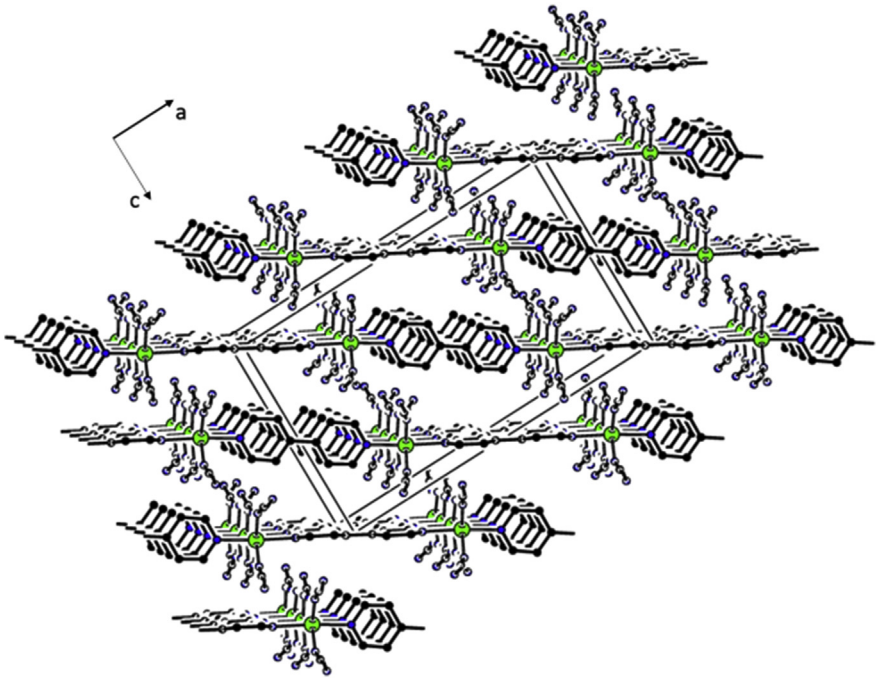

Fig. 4. 2-D network structure of complex 2 in the ac-plane. H atoms, ethanol molecules and free bpy ligands have been omitted for clarity.

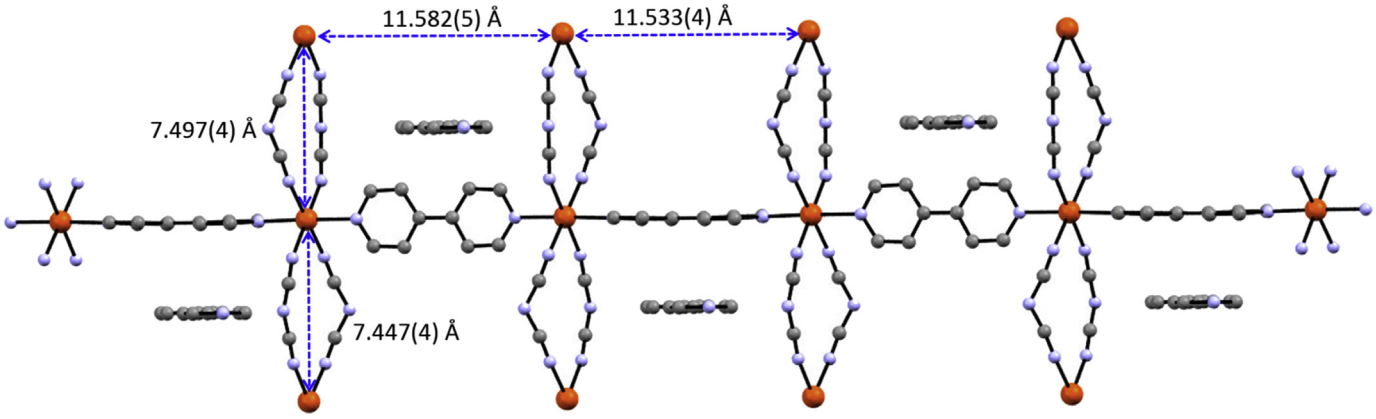

Fig. 5. 1-D chain extension along the [101]. Ethanol molecules and hydrogen atoms are omitted for clarity.

partitioning of space into regions where the electron density $\rho_{int}(\mathbf{r})$ of the promolecule is larger than $\rho_{ext}(\mathbf{r})$ of the surrounding molecules, yields the so-called Hirshfeld surface, where $\rho_{int}(\mathbf{r})/[\rho_{int}(\mathbf{r}) + \rho_{ext}(\mathbf{r})] = 0.5$. This surface is representative of the region in space where intermolecular interactions take place [43]. Therefore, quantitative insights into the chemical nature of intermolecular interactions in the crystalline state can be obtained by its analysis. The shape of the Hirshfeld surface around a metal is flat in the regions of interactions. For organometallic compounds it depends on the coordination of the metal atom [44–46].

The Fe(II) cation atom is located on a two-fold symmetry axis and its shape is cuboid (Fig. 6), as there are six nitrogen ligands arranged in a distorted octahedral coordination geometry.

Some N–Fe–N angles deviate significantly from 90° with N11–Fe1–N11^{i} (1 - x, y, -z + ½) only at 74.16(8)° (Table S1). The Fe(II) cation follows a crystallographic symmetry which renders its shape more regular [45]. The electron density on the surface is highest in the directions of the coordination bonds (Fig. 6) and reaches 0.20 e/Å^3.

The C atoms constitute the most abundant species, occupying 36.5% of the Hirshfeld surface, followed by hydrogen, nitrogen and iron. Hydrophobic contacts involving H and C atoms constitute slightly more than half of the entire contact surface. H···C interactions at 37.5% is the most abundant.

A contact enrichment ratio larger than unity for a given pair of chemical species indicates that these contacts are over-represented in the crystal packing when compared to equiprobable contacts computed from the chemical composition on the Hirshfeld surface [47]. The Fe···N coordination interaction is the most over-represented contact at $E = 3.5$ and represent as much as 23.8% of the contact surface (Table 2).

All self-contacts are generally avoided, except C···C due to extensive π···π stacking occurring between the organic cations.

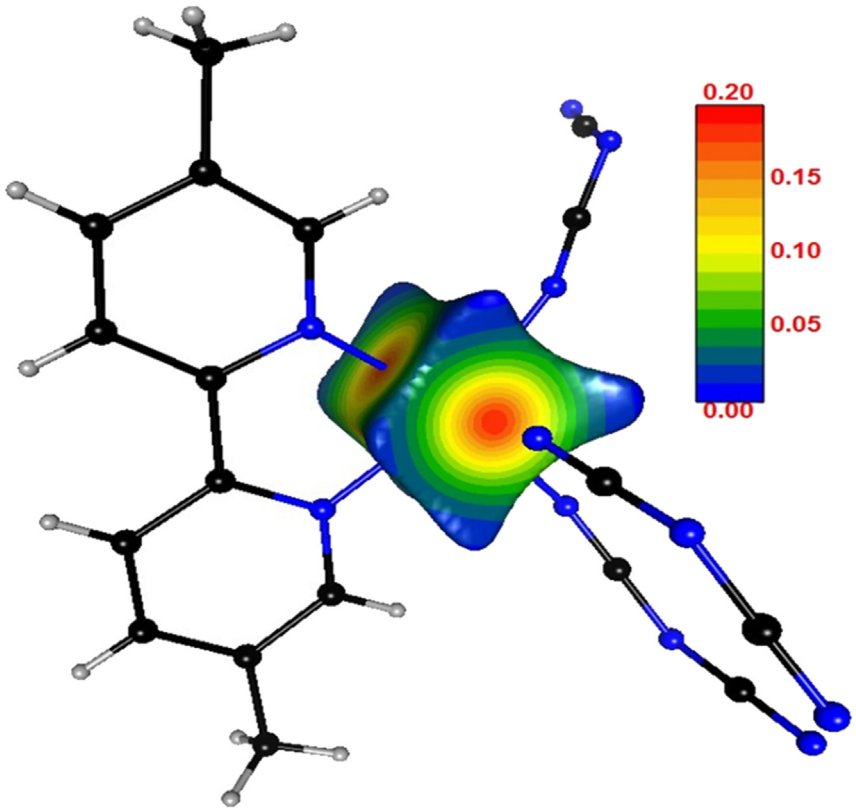

Fig. 6. Hirshfeld surface around the ensemble of Fe cation coordinated by six nitrogen atoms: two from dmbpy and four N atoms from Dicyanamide. The surface is colored according to the electron density (e/Å^3).

Table 2
Statistical analysis of intermolecular contacts in compound **1**. The Hirshfeld surface was computed as in Fig. 6 with the program MoProViewer [48]. The second row shows the chemical content on the Hirshfeld surface, followed by the percentage C_{xy} of the actual contact types and their Enrichments E_{xy}. The major contacts and the most enriched are highlighted in bold.

Complex 1	C	N	Fe	Hc
surface %	36.5	26.2	8.2	29.0
C	12.6			
N	6.1	1.4		contacts %
Fe	2.1	23.8	0.0	
Hc	37.5	12.7	2.4	1.4
C	1.00			
N	0.38	0.28		enrichment
Fe	0.21	3.5	0.00	
Hc	1.9	1.02	0.30	0.19

Compound **1** has only H–C type hydrogen atoms. Hc···Hc contacts are very under-represented in the crystal packing due to competition with CH···N hydrogen bonding with dicyanamide and the electrostatically more attractive C···Hc weak H-bonds.

In conclusion, the most enriched contacts are the Fe···N coordination interactions followed by the CH···C hydrophobic π interactions (considered as weak hydrogen bonds), while the stronger CH···N hydrogen bonds are not over-represented.

Compound 2. The Fe(II) cation atom is located on a regular position with six different nitrogen atoms as ligand and the shape of its Hirshfeld surface is cuboid (Fig. 7).

The six nitrogen ligands are arranged in slightly distorted octahedral coordination geometry. The N–Fe–N angles deviating most from 90° are N51–Fe–N61 = 85.95(11)° and N41–Fe–N51 = 94.64(11)° (Table S2). The electron density on the Hirshfeld surface can be seen in Fig. 8 and reach 0.20 e/Å^3 in the directions of the coordination bonds.

The C atoms constitute the most abundant species, occupying 36.5% of the Hirshfeld surface, followed by hydrogen, nitrogen and iron (Table 3). Hydrophobic contacts involving Hc and C atoms constitute around 40% of the entire contact surface. Hc ··· C interactions at 21.5% are the most abundant together with the Fe···N coordination interaction. The Fe···N contact is the most over-represented at $E = 3.05$ and the Fe atom contact surface is made almost exclusively of nitrogen atoms.

All self-contacts are generally avoided, except C···C due to extensive π···π stacking occurring between the organic cations. Hc···Hc contacts are slightly under-represented in the crystal packing due to competition with C–H···N hydrogen bonding with dicyanamide and the electrostatically more attractive C···Hc weak π interactions.

The ethanol molecule is disordered and in the main conformation, the O–Ho hydroxyl group forms weak interactions with Hc-C atoms. The role of the solvent molecule is more to fill a void in the crystal packing than to make strong interacting.

In both compound, the most enriched contacts are the Fe···N coordination interactions followed by the hydrophobic C···Hc contacts. The stronger Hc···N hydrogen bonds are not over-represented in **1** and even moderately avoided in compound **2**, presumably due to competition with Fe···N coordination. The major differences between the two compounds occur in the balance between the different hydrophobic interactions. Hc···Hc interactions are much less under-represented ($E = 0.93$ vs. 0.19) and C···C contacts are more favored in **2** compared to **1**. Conversely, Hc···C contacts are much more enriched in **2** compared to **1** ($E = 1.9$ vs 1.5).

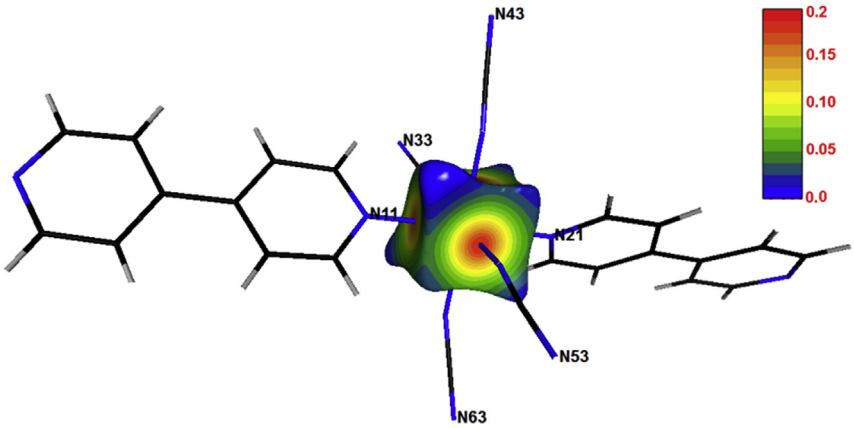

Fig. 7. Hirshfeld surface around the Fe cation, coordinated by six nitrogen atoms. The surface is colored according to the electron density (e/Å^3).

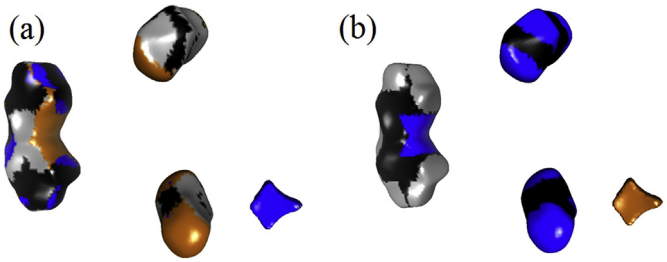

Fig. 8. Hirshfeld surface around one Fe cation, two dicyanamide and one dmbpy molecules (two copies of the asymmetric unit). (a) The surface is colored according to the interior atom contributing most to the electron density. (b) Coloring according to the exterior contact atoms. In order to obtain integral surfaces, moieties not in contact with each other were selected in the crystal. H: grey, C: black, N: blue, Fe: orange. (For interpretation of the references to color in this figure legend, the reader is referred to the Web version of this article.)

Table 3
Chemical proportions on the Hirshfeld surface of the entities constituting the crystal structure of compound **2**. Only the conformer of ethanol with largest occupancy was kept. Ho and Hc correspond to hydrogen atoms bound to oxygen and carbon, respectively.

Atom	Ho	C	N	O	Fe	Hc
%	1.5	36.5	27.7	1.4	7.5	25.4
Ho	0.0					
C	0.7	**13.9**			contacts %	
N	0.1	8.5	**8.6**			
O	0.0	0.9	0.4	0.0		
Fe	0.0	2.1	**21.7**	0.0	0.0	
Hc	3.9	**21.7**	**10.1**	1.5	1.2	4.7
HO	0.00					
C	0.5	**1.5**			enrichment	
N	0.05	0.47	1.0			
O	0.0	1.1	0.44	0.0		
Fe	0.0	0.25	**3.0**	0.0	0.01	
Hc	3.4	**1.5**	0.73	2.3	0.19	0.83

4. Conclusions

In this work, synthesis, single crystal X-ray structure analyses and characterization of two new dicyanamide bridged Fe(II) coordination polymers, **1** and **2**, containing 5,5′-dimethyl-bipyridine and 4,4′-bipyridine ligands, respectively, have been reported. The structural analysis of both complexes shows that the environment around the six-coordinated Fe(II) ion can be described as a slightly distorted octahedral geometry and the dca ligand is coordinated to the metal site in a bidentate $\mu_{1,5}$-bridging mode to form 1-D coordination polymer. In complex **2**, these polymeric chains are also linked with bpy ligands to form 2-D layers. The selection of 4,4′-bpy and dmbpy as co-ligand has a rather important role in the crystal structure arrangement of dca coordination polymers due to their various coordination modes and bridging ability. Using dca ligand with dmbpy instead of 4,4′-bpy ligand leads to absolutely different network in compound **1** which is a rare example in which end-to-end double bridged dca ligands and bidentate bulky aromatic ligands are coordinated simultaneously to the metal center. Statistical analysis of contacts confirms that the Fe···N coordination contacts are the most enriched and constitute the first drive force in both crystal packings. Hydrophobic forces, involving Hc and C atoms, play also a big role in the crystal arrangements but the balance between these contacts types is different in the two compounds.

Acknowledgements

The authors are indebted to the Algerian DG-RSDT (Direction Générale de la Recherche Scientifique et du Développement Technologique) and Université Ferhat Abbas Sétif 1. M.M. is grateful to Ferdowsi University of Mashhad Research Council for their financial support of this work.

Appendix A. Supplementary data

Supplementary data related to this article can be found at https://doi.org/10.1016/j.molstruc.2018.07.049.

References

[1] C. Genre, E. Jeanneau, A. Bousseksou, D. Luneau, S.A. Borshth, G.S. Matouzenko, First dicyanamide-bridged spin-crossover coordination polymer: synthesis, structural, magnetic, and spectroscopic studies, Chem. Eur J. 14 (2008) 697–705, https://doi.org/10.1002/chem.200700998.
[2] J. Carranza, C. Brennan, J. Sletten, F. Lloret, M. Julve, Three one-dimensional systems with end-to-end dicyanamide bridges between copper(ii) centres: structural and magnetic properties, J. Chem. Soc. Dalton Trans. (2002) 3164–3170, https://doi.org/10.1039/b203085n.
[3] Q. Li, H.-T. Wang, A new three-dimensional anionic cadmium(II) dicyanamide network, Acta Crystallogr. Section C Struct. Chem. 70 (2014) 1054–1056, https://doi.org/10.1107/S2053229614022360.

[4] S. Triki, F. Thétiot, J.-R. Galán-Mascarós, J. Sala Pala, K.R. Dunbar, New compounds with bridging dicyanamide and bis-chelating 2,2'-bipyrimidine ligands: syntheses, structural characterisation and magnetic properties of the two-dimensional materials $[Fe_2(dca)_4(bpym)]\cdot H_2O$ and $[Fe_2(dca)_4(bpym)(H_2O)_2]$, N. J. Chem. 25 (2001) 954–958, https://doi.org/10.1039/b102188p.

[5] S. Benmansour, C. Atmani, F. Setifi, S. Triki, M. Marchivie, C.J. Gómez-García, Polynitrile anions as ligands: from magnetic polymeric architectures to spin crossover materials, Coord. Chem. Rev. 254 (2010) 1468–1478, https://doi.org/10.1016/j.ccr.2009.11.011.

[6] S. Benmansour, F. Setifi, S. Triki, J.-Y. Salaün, F. Vandevelde, J. Sala-Pala, C.J. Gómez-García, T. Roisnel, New multidimensional coordination polymers with μ2- and μ3-dcno cyano carbanion ligand {dcno− = $[(NC)_2CC(O)O(CH_2)_2OH]^-$}, Eur. J. Inorg. Chem. 2007 (2007) 186–194, https://doi.org/10.1002/ejic.200600449.

[7] A. Miyazaki, K. Okabe, T. Enoki, F. Setifi, S. Golhen, L. Ouahab, T. Toita, J. Yamada, Weak ferromagnetism of (BDH-TTP)$[M(isoq)_2(NCS)_4]$ (M = Cr), Synth. Met. 137 (2003) 1195–1196, https://doi.org/10.1016/S0379-6779(02)00980-3.

[8] F. Setifi, E. Milin, C. Charles, F. Thétiot, S. Triki, C.J. Gómez-García, Spin crossover Iron(II) coordination polymer chains: syntheses, structures, and magnetic characterizations of $[Fe(aqin)_2(\mu_2\text{-}M(CN)_4)]$ (M = Ni(II), Pt(II), aqin = Quinolin-8-amine), Inorg. Chem. 53 (2014) 97–104, https://doi.org/10.1021/ic401721x.

[9] Z. Setifi, F. Setifi, L. El Ammari, M. El-Ghozzi, J. Sopková-de Oliveira Santos, H. Merazig, C. Glidewell, Poly[[chlorido(1,10-phenanthroline-κ 2N, N')copper(II)]-μ3 -1,1,3,3-tetracyano-2-ethoxypropenido-κ 3N :: N': N']: coordination polymer sheets linked into bilayers by hydrogen bonds, Acta Crystallogr. Section C Struct. Chem. 70 (2014) 19–22, https://doi.org/10.1107/S2053229613032804.

[10] C. Yuste, A. Bentama, N. Marino, D. Armentano, F. Setifi, S. Triki, F. Lloret, M. Julve, Copper(II) complexes with 2,5-bis(2-pyridyl)pyrazine and 1,1,3,3-tetracyano-2-ethoxypropenide anion: syntheses, crystal structures and magnetic properties, Polyhedron 28 (2009) 1287–1294, https://doi.org/10.1016/j.poly.2009.02.029.

[11] S. Benmansour, F. Setifi, S. Triki, C.J. Gómez-García, Linkage isomerism in coordination polymers, Inorg. Chem. 51 (2012) 2359–2365, https://doi.org/10.1021/ic202361p.

[12] E. Gungor, Y. Yahsi, H. Kara, A. Caneschi, The first 3D and trinuclear cyano-bridged FeII–FeIII $(CN)_6$ complexes: structure and magnetic characterizations, CrystEngComm 17 (2015) 3082–3088, https://doi.org/10.1039/C5CE00261C.

[13] U. Erkarslan, G. Oylumluoglu, M.B. Coban, E. Öztürk, H. Kara, Cyanide-bridged trinuclear MnIII–FeIII assembly: crystal structure, magnetic and photoluminescence behavior, Inorg. Chim. Acta. 445 (2016) 57–61, https://doi.org/10.1016/j.ica.2016.02.010.

[14] H. Kara, A. Azizoglu, A. Karaoglu, Y. Yahsi, E. Gungor, A. Caneschi, L. Sorace, Synthesis, crystal structure, magnetic properties and computational study of a series of cyano-bridged MnIII-FeIII complexes, CrystEngComm 14 (2012) 7320, https://doi.org/10.1039/c2ce25646k.

[15] Z. Setifi, B. Gaamoune, H. Stoeckli-Evans, D.-A. Rouag, F. Setifi, A new coordination complex based on a polynitrile ligand: bis(4-amino-3,5-di-2-pyridyl-4H -1,2,4-triazole)diaquairon(II) bis(1,1,3,3-tetracyano-2-methylsulfanylpropenide), Acta Crystallogr. Sect. C Cryst. Struct. Commun. 66 (2010) m286–m289, https://doi.org/10.1107/S010827011003578X.

[16] Z. Setifi, M. Ghazzali, C. Glidewell, O. Pérez, F. Setifi, C.J. Gómez-García, J. Reedijk, Azide, water and adipate as bridging ligands for Cu(II): synthesis, structure and magnetism of (μ_4-adipato-κ-O)(μ-aqua)(μ-azido-κN1,N 1) copper(II) monohydrate, Polyhedron 117 (2016) 244–248, https://doi.org/10.1016/j.poly.2016.05.060.

[17] M.K. Urtiaga, M.G. Barandika, M.I. Arriortua, N. De Pinta, S. Martı, L. Lezama, G. Madariaga, R. Cort, D. De Quı, F. De Farmacia, Structural analysis, Spectroscopic, and magnetic properties of the 1D Triple-Bridged Compounds $[M(dca)_2(bpa)]$ (M =Mn, Fe, Co, Zn; dca = dicyanamide ; bpa =1, 2-bis(4-pyridyl) ethane) and the 3D $[Ni(dca)(bpa)_2]dca_3$ $6H_2O$, Inorg. Chem. 2 (2010) 10445–10454, https://doi.org/10.1021/ic1014626.

[18] D.S. Tonzing, S.R. Batten, K.S. Murray, 1D chain structures of $M(dca)_2$(-phen)(H_2O) MeOH, M Z Mn, Fe, Co, Ni, Zn, Cd, dca dicyanamide, $N(CN)K_2$, phen, 7-phenanthroline, J. Mol. Struct. 796 (2006) 63–68, https://doi.org/10.1016/j.molstruc.2006.03.033.

[19] A.M. Kutasi, A.R. Harris, S.R. Batten, B. Moubaraki, K.S. Murray, Coordination polymers of dicyanamide and Methylpyrazine: syntheses, structures, and magnetic properties, Cryst. Growth Des. 4 (2004) 605–610, https://doi.org/10.1021/cg049952x.

[20] A. Mirzaei, H. Eshtiagh-Hosseini, Z. Bolouri, Z. Rahmati, M.B. Esmaeilzadeh, A. Hassanpoor, A. Bauza, P. Ballester, A.F. Oliver, J.T. Mague, B. Notash, Rationalization of noncovalent interactions within six new MII/8-aminoquinoline Supramolecular complexes (MII = Mn, Cu, and Cd): a combined experimental and theoretical DFT study, Cryst. Growth Des. 15 (2015) 1351–1361, https://doi.org/10.1021/cg501752e.

[21] J.L. Manson, A.M. Arif, C.D. Incarvito, L.M. Liable-Sands, A.L. Rheingold, J.S. Miller, Structures and magnetic properties of novel 1-d coordination polymers containing both dicyanamide and pyridine-type ligands, J. Solid State Chem. 145 (1999) 369–378, https://doi.org/10.1006/jssc.1998.8059.

[22] A. Claramunt, A. Escuer, F. a. Mautner, N. Sanz, R. Vicente, Two new one-dimensional systems with end-to-end single dicyanamide bridges between manganese(II) centres: structural and magnetic properties, J. Chem. Soc. Dalton Trans. (2000) 2627–2630, https://doi.org/10.1039/b002214o.

[23] J.L. Manson, D.W. Lee, A.L. Rheingold, J.S. Miller, Buckled-layered structure of zinc dicyanamide, $Zn^{II}[N(CN)_2]_2$, Inorg. Chem. 37 (1998) 5966–5967, https://doi.org/10.1021/ic980659u.

[24] J.L. Manson, C.D. Incarvito, A.L. Rheingold, J.S. Miller, Structure and magnetic properties of MnII[N(CN)2]2(pyrazine). An antiferromagnet with an interpenetrating 3-D network structure, J. Chem. Soc., Dalton Trans. (1998) 3705–3706, https://doi.org/10.1039/a807788f.

[25] P. Jensen, S.R. Batten, G.D. Fallon, D.C.R. Hockless, B. Moubaraki, K.S. Murray, R. Robson, Synthesis, structural isomerism, and magnetism of extended framework compounds of type [Cu (dca)$_2$(pyz)]n, where dca=Dicyanamide ($N(CN)^{-2}$) and pyz=Pyrazine, J. Solid State Chem. 145 (1999) 387–393, https://doi.org/10.1006/jssc.1998.8082.

[26] J.L. Manson, A.M. Arif, J.S. Miller, Crystal structure and magnetic properties of $[Fe\{N(CN)_2\}_2(MeOH)_2]$ a 2-D layered network consisting of hydrogen-bonded 1-D chains, J. Mater. Chem. 9 (1999) 979–983, https://doi.org/10.1039/a808089e.

[27] S.R. Batten, P. Jensen, C.J. Kepert, M. Kurmoo, B. Moubaraki, K.S. Murray, D.J. Price, Syntheses, structures and magnetism of α-$Mn(dca)_2$, $[Mn(dca)_2(H_2O)_2]\cdot H_2O$, $[Mn(dca)_2(C_2H_5OH)_2]\cdot(CH_3)_2CO$, $[Fe(dca)_2(CH_3OH)_2]$ and $[Mn(dca)_2(L)_2]$, where L = pyridine, CH_3OH or DMF and dca^- = dicyanamide, $N(CN)^{2-}$, J. Chem. Soc. Dalton Trans. (1999) 2987–2997, https://doi.org/10.1039/a903487k.

[28] S.R. Batten, K.S. Murray, Structure and magnetism of coordination polymers containing dicyanamide and tricyanomethanide, Coord. Chem. Rev. 246 (2003) 103–130, https://doi.org/10.1016/S0010-8545(03)00119-X.

[29] L.B. Lopes, C.C. Corrêa, G.P. Guedes, M.G.F. Vaz, R. Diniz, F.C. Machado, Two new coordination polymers involving Mn(II), Co(II), dicyanamide anion and the nitrogen ligand 5,5'-dimethyl-2,2'-dipyridine: crystal structures and magnetic properties, Polyhedron 50 (2013) 16–21, https://doi.org/10.1016/j.poly.2012.10.032.

[30] S. Konar, U. Saha, M. Dolai, S. Chatterjee, Synthesis of 2D polymeric dicyanamide bridged hexa-coordinated Cu(II) complex: structural characterization, spectral studies and TDDFT calculation, J. Mol. Struct. 1075 (2014) 286–291, https://doi.org/10.1016/j.molstruc.2014.06.080.

[31] M. Biswas, S.R. Batten, P. Jensen, S. Mitra, Retention of (4,4) connectivity in the absence of $\pi\cdots\pi$ interactions in a cadmium tris-dicyanamide compound, Aust. J. Chem. 59 (2006) 115–117, https://doi.org/10.1071/CH05315.

[32] U. Bruker, APEX2, SADABS and SAINT, Bruker AXS Inc., Madison, Wisconsin, 2013.

[33] G.M. Sheldrick, A short history of SHELX, Acta Cryst. A. 64 (2008) 112–122, https://doi.org/10.1107/S0108767307043930.

[34] G.M. Sheldrick, Crystal structure refinement with SHELXL, Acta cryst. C 71 (2015) 3–8, https://doi.org/10.1107/S2053229614024218.

[35] F. Reuter, E. Rentschler, Structural, magnetic and electronic characterization of an isostructural series of dinuclear complexes of 3d metal ions bridged by tpbd, Polyhedron 52 (2013) 788–796, https://doi.org/10.1016/j.poly.2012.07.050.

[36] F. Setifi, P. Konieczny, C. Glidewell, M. Arefian, R. Pelka, Z. Setifi, M. Mirzaei, Synthesis, structure, and magnetic properties of a dinuclear antiferromagnetically coupled iron(II) complex, J. Mol. Struct. 1149 (2017) 149–154, https://doi.org/10.1016/j.molstruc.2017.07.085.

[37] Z. Setifi, F. Setifi, S.W. Ng, A. Oudahmane, M. El-Ghozzi, D. Avignant, Tris(1,10-phenanthroline-κ 2 N, N')iron(II) bis(1,1,3,3-tetracyano-2-ethoxypropenide) hemihydrate, Acta Crystallogr. Section E Struct. Rep. 69 (2013) m12–m13, https://doi.org/10.1107/S1600536812048611. Online.

[38] Z. Setifi, K.V. Domasevitch, F. Setifi, P. Mach, S.W. Ng, V. Petříček, M. Dušek, Multiple anion$\cdots\pi$ interactions in tris(1,10-phenanthroline-κ2 N,N')iron(II) bis[1,1,3,3-tetracyano-2-(2-hydroxyethyl)propenide] monohydrate, Acta Crystallogr. Sect. C Cryst. Struct. Commun. 69 (2013) 1351–1356, https://doi.org/10.1107/S0108270113027108.

[39] Z. Setifi, F. Setifi, H. Boughzala, A. Beghidja, C. Glidewell, Tris(2,2'-bipyridine) iron(II) bis(1,1,3,3-tetracyano-2-ethoxypropenide) dihydrate: chiral hydrogen-bonded frameworks interpenetrate in three dimensions, Acta Crystallogr. Section C Struct. Chem. 70 (2014) 465–469, https://doi.org/10.1107/S2053229614008092.

[40] R.D. Shannon, C.T. Prewitt, Effective ionic radii in oxides and fluorides, Acta Crystallogr. Sect. B Struct. Crystallogr. Cryst. Chem. 25 (1969) 925–946, https://doi.org/10.1107/S0567740869003220.

[41] A.B. Gaspar, M.C. Muñoz, J.A. Real, Clathration effects on the interpenetration in the 2D (4,4) coordination polymer {[Fe(4,4'-bipy)(dca)2]}, Inorg. Chem. Commun. 7 (2004) 815–817, https://doi.org/10.1016/j.inoche.2004.05.005.

[42] J.-H. Luo, M.-C. Hong, R. Cao, Y.-C. Liang, Y.-J. Zhao, R.-H. Wang, J.-B. Weng, Syntheses and crystal structures of cadmium(II) coordination polymers with end-to-end dicyanamide bridges, Polyhedron 21 (2002) 893–898, https://doi.org/10.1016/S0277-5387(02)00868-9.

[43] M.A. Spackman, P.G. Byrom, A novel definition of a molecule in a crystal, Chem. Phys. Lett. 267 (1997) 215–220, https://doi.org/10.1016/S0009-2614(97)00100-0.

[44] I. Skovsen, M. Christensen, H.F. Clausen, J. Overgaard, C. Stiewe, T. Desgupta, E. Mueller, M.A. Spackman, B.B. Iversen, Synthesis, crystal structure, atomic Hirshfeld surfaces, and physical properties of hexagonal CeMnNi 4, Inorg. Chem. 49 (2010) 9343–9349, https://doi.org/10.1021/ic100990a.

[45] M.R.V. Jørgensen, I. Skovsen, H.F. Clausen, J.-L. Mi, M. Christensen, E. Nishibori, M.A. Spackman, B.B. Iversen, Application of atomic Hirshfeld surface analysis to intermetallic systems: is Mn in cubic $CeMnNi_4$ a thermoelectric rattler atom? Inorg. Chem. 51 (2012) 1916–1924, https://doi.org/10.1021/ic202231k.

[46] A.V. Vologzhanina, A.A. Korlyukov, V.V. Avdeeva, I.N. Polyakova, E.A. Malinina, N.T. Kuznetsov, Theoretical QTAIM, ELI-D, and Hirshfeld surface analysis of the Cu–(H)B interaction in $[Cu_2($ bipy $)_2B_{10}H_{10}]$, J. Phys. Chem. 117 (2013) 13138–13150, https://doi.org/10.1021/jp405270u.

[47] C. Jelsch, K. Ejsmont, L. Huder, The enrichment ratio of atomic contacts in crystals, an indicator derived from the Hirshfeld surface analysis, IUCrJ 1 (2014) 119–128, https://doi.org/10.1107/S2052252514003327.

[48] C.J.B. Guillot, E. Enrique, L. Huder, A tool to study proteins from a charge density science perspective, Acta Cryst. A (2014) C279.